Analysis of Off-Board Powered Thermal Preconditioning in Electric Drive Vehicles

Preprint

Robb A. Barnitt, Aaron D. Brooker,
Laurie Ramroth, John Rugh, and
Kandler A. Smith

Presented at the 25th World Battery, Hybrid and Fuel Cell Electric Vehicle Symposium & Exhibition
Shenzhen, China
November 5 – 9, 2010

NREL is a national laboratory of the U.S. Department of Energy, Office of Energy Efficiency & Renewable Energy, operated by the Alliance for Sustainable Energy, LLC.

Conference Paper
NREL/CP-5400-49252
December 2010

Contract No. DE-AC36-08GO28308

Available electronically at http://www.osti.gov/bridge

Available for a processing fee to U.S. Department of Energy
and its contractors, in paper, from:

U.S. Department of Energy
Office of Scientific and Technical Information

P.O. Box 62
Oak Ridge, TN 37831-0062
phone: 865.576.8401
fax: 865.576.5728
email: mailto:reports@adonis.osti.gov

Available for sale to the public, in paper, from:

U.S. Department of Commerce
National Technical Information Service
5285 Port Royal Road
Springfield, VA 22161
phone: 800.553.6847
fax: 703.605.6900
email: orders@ntis.fedworld.gov
online ordering: http://www.ntis.gov/help/ordermethods.aspx

Cover Photos: (left to right) PIX 16416, PIX 17423, PIX 16560, PIX 17613, PIX 17436, PIX 17721

Printed on paper containing at least 50% wastepaper, including 10% post consumer waste.

Analysis of Off-Board Powered Thermal Preconditioning in Electric Drive Vehicles

Robb A. Barnitt, Aaron D. Brooker, Laurie Ramroth, John Rugh, and Kandler A. Smith

National Renewable Energy Laboratory, 1617 Cole Blvd., Golden, CO 80401, U.S.A.
E-mail: robb.barnitt@nrel.gov

Abstract—Following a hot or cold thermal soak, vehicle climate control systems (air conditioning or heat) are required to quickly attain a cabin temperature comfortable to the vehicle occupants. In a plug-in hybrid electric or electric vehicle (PEV) equipped with electric climate control systems, the traction battery is the sole on-board power source. Depleting the battery for immediate climate control results in a reduced charge-depleting (CD) range and additional battery wear. PEV cabin and battery thermal preconditioning using off-board power supplied by the grid or a building can mitigate the CD range reduction and battery life impacts of climate control. To quantify the impact, the National Renewable Energy Laboratory (NREL) applied the Powertrain Systems Analysis Toolkit vehicle simulation program to develop and validate models of three relevant PEV platforms: a blended plug-in hybrid electric vehicle (PHEV) with a 15-mile (24-km) electric range (PHEV15), a series PHEV with a 40-mile (64-km) electric range (PHEV40s), and an electric vehicle with a 100-mile (161-km) electric range (EV). Second, NREL surveyed literature and test data to develop representative air conditioning and heater load profiles. Next, NREL simulated PEV performance with and without thermal preconditioning over the UDDS and HWFET drive cycles, and for three different ambient temperature scenarios. Finally, battery wear was characterized using a physically justified semi-empirical lithium ion battery life model. This analysis shows that climate control loads can reduce CD range up to 35%. However, cabin thermal preconditioning can increase CD range up to 19% when compared to no thermal preconditioning. In addition, this analysis shows that while battery capacity loss over time is driven by ambient temperature rather than climate control loads, concurrent battery thermal preconditioning can reduce capacity loss up to 7% by reducing pack temperature in a high ambient temperature scenario.

Keywords— EV, PEV, PHEV, thermal, climate control

1. Introduction

Production and sales of plug-in hybrid electric and electric vehicles are forecasted to increase in the coming years. PEVs are viewed as a means to reduce liquid petroleum fuel consumption by using a greater fraction of electrical energy supplied by an on-board battery. The charge-depleting (CD) range of a PEV is limited by on-board battery capacity, which is used not only for driving but also other loads. Notably, climate control loads (heating and cooling) can reduce the PEV's CD range and/or cause the internal combustion engine to operate more frequently. Climate control loads increase PEV operating costs (liquid fuel and battery wear) and diminish the PEV's intended usability (decreased CD range). PEVs represent a unique opportunity to thermally precondition a vehicle when it is plugged into an off-board power source. During hot or cold weather, the climate control load on the on-board power source is high at startup to cool down or warm up the vehicle from a thermal-soaked condition to a comfortable condition. If the cool down or warm up can be accomplished during battery charging, the higher transient climate control load on the power source could be eliminated. The reduction of the climate control load due to preconditioning has the potential to reduce fuel consumption and partially restore CD range. Additional advantages include improved battery life, improved occupant thermal comfort, and potentially improved safety due to enhanced driver vigilance.

2. Project Approach

This section describes the approach to vehicle selection, model development and validation, fuel economy calculation, climate control load profile development, battery life modeling, and climate control scenarios.

2.1 Vehicle Selection

PEVs that operate in CD mode at the beginning of a trip can potentially benefit from off-board powered thermal preconditioning. The most relevant PEV platforms that are scheduled for near-term market release are:

1. PHEV15—a blended PHEV with an approximately 15-mile (23.4-km) all-electric range (AER) under certain usage conditions.
2. PHEV40s—a series PHEV designed to provide up to 40 miles (64 km) of AER, then operate in charge-sustaining (CS) mode using a range-extending gasoline engine.
3. EV—an EV designed to provide up to 100 miles of AER.

All three PEVs use electric heating and cooling climate control systems.

2.2 Vehicle Model Development

Vehicle models were assembled using the Powertrain Systems Analysis Toolkit (PSAT). Relevant vehicle model specifications for each vehicle platform are presented in Table 1.

Table 1: Vehicle Model Inputs

	PHEV15	PHEV40s	EV
C_d	0.25	0.28	0.29
Frontal Area (m^2)	2.07	2.09	2.33
Vehicle Mass (kg)	1,490	1,588	1,271
Engine Power (kW)	73	53	NA
Motor Power (kW)	60, 42	100	80
Battery Capacity (kWh)	5.2	16	24
Battery Delta State of Charge (SOC)	66%	54%	84%
Battery Maximum SOC	80%	80%	95%
Battery Thermal Management Strategy	Air cooling	Liquid cooling	No active cooling
Battery Heat Transfer Coefficient (W/m^2K)	20	110	0
Accessory Load (W)	300	300	300

2.3 Vehicle Model Validation

Once assembled, the models were validated based on fuel consumption in CS mode, CD range, and acceleration performance. Generally, the simulated results fell within 10% of the published data (Table 2).

Table 2: Vehicle Model Validation Results

	PHEV15	PHEV40s	EV
CD Range (km)			
Published	23.4	64.4	160.9
Simulated	24.9	66.3	168.8
Error	+6.6%	+3.0%	+4.9%
Fuel Consumption CS Mode (L/100km)			
Published	3.27	4.70	NA
Simulated	3.42	4.39	NA
Error	+4.59%	-6.60%	
0-60 mph Acceleration			
Published	10.9	8.5	NA
Simulated	9.6	8.9	NA
Error	-11.9%	+4.7%	

2.4 Fuel Economy and CD Range Calculations

A series of steps is used to estimate conventional and hybrid electric vehicle fuel economy. Before 2008, the U.S. Environmental Protection Agency (EPA) estimated vehicle fuel economy using two cycles, one representing city driving, and the other representing highway driving. Since these tests underestimated the amount of fuel use consumers would typically experience, each test result was multiplied by an adjustment factor. A weighted average was then used to combine the two adjusted test results.

In 2008, three more cycles were added to the test procedure to improve the fuel economy estimate. The five-cycle test procedure would take especially long to run for PHEVs. PHEVs have two fuel economies that characterize their performance on a drive cycle, the CD fuel economy and the charge sustaining (CS) fuel economy. Both estimates are needed to calculate a combined average based on how much driving is done in each mode. To calculate the two fuel economies, each drive cycle must be repeated until the vehicle depletes the battery and runs one complete CS mode cycle. Repeating five cycles multiple times is computationally intensive.

EPA derived a two-cycle approximation of the five-cycle test, as seen below in equations (1) and (2). This was used in this study to reduce computational time. For the PHEVs, the two-cycle approximation is used for CD mode and CS mode, as described in [1]. A weighted average of the two different mode fuel economies is then calculated based on statistics that show the distance typically driven in each mode.

$$City\ MPG = 1/(.003259 + \frac{1.1805}{City\ MPG}) \quad (1)$$

$$Highway\ MPG = 1/(.001376 + \frac{1.3466}{HFET\ MPG}) \quad (2)$$

The CD range estimate used for the fuel economy calculation would not work for this study. It is based on discrete cycle increments, which would not capture the shorter cycle changes caused by preconditioning. Instead, this study used SOC values to estimate the CD range. Specifically, the CD distance was defined as the distance at which the SOC first reaches the average CS SOC plus 1%. One percent SOC was added to the average CS SOC to improve the consistency of the method. Without the addition, the CD range did not consistently line up well with where the SOC leveled out.

A similar approach was used to estimate the range of the EV. This approach also used the two-cycle approximation of the five-cycle test procedure. Also, like the way each cycle was repeated multiple times for the PHEVs to estimate CD and CS mode fuel economies, the cycles were repeated twice for the EV to account for the higher heating or A/C load during the first cycle. Each depletion rate was then converted to a miles per gallon gasoline equivalent and adjusted using the two-cycle approximation equations. Unlike the PHEVs, a 30% fuel consumption adjustment ceiling was used to prevent the equations from extrapolating too far outside their intended domain. The two adjusted cycle consumption rates were then averaged based on the distance that would be driven in each mode, similar to how the CS and CD modes were averaged for PHEVs. Finally, the averaged adjusted city and highway results were average-weighted 55% and 45%, respectively, to come to a single fuel consumption rate. This rate was then multiplied by the usable capacity to estimate the total range.

2.5 Climate Control Loads

A climate control load is divided into two parts:

1. Transient—After a thermal soak, the transient climate control is characterized by a high initial load that decreases with time. An example is entering a hot vehicle after parking in the sun, driving, and having the air conditioning (A/C) on with maximum blower airflow to cool the interior. Vehicles have different transient times due to a variety of factors based on

manufacturer design choices. We selected 10 minutes as a representative transient duration.

2. Steady State—During steady state, the impact of the thermal soak has been diminished. The climate control system maintains the thermal conditions in the passenger compartment. An example is driving down the interstate in the winter and having a moderate heat setting with the blower on low.

Thermal preconditioning eliminates the transient climate control load on the battery. In this situation, the on-board power supply has only to provide the steady-state climate control load. We surveyed literature and test data to develop representative A/C and heater load profiles for our simulation vehicles.

2.5.1 Cooling

For the A/C load, we constructed a load vs. time profile that was representative across our range of vehicles. Table 3 shows the range of vehicle types, environments, and A/C systems from a variety of sources that we considered.

Table 3: Cooling Load Data Sources

Source	Vehicle	Environment	A/C
SAE ARCRP [2]	N/A, bench data	hot	mechanical
ANL [3]	small EV	moderate	electrical
NREL [4]	Prius	hot	electrical
Ford [5]	Fusion	hot	electrical
ANL [3]	Mercedes S400	moderate	electrical
Visteon [6]	midsized SUV	hot	mechanical

The data from these sources were averaged to create a composite load profile. The 10-minute transient load was applied to the model as a linear decay from a peak power of 3.89 kW at the start of the drive to a 2.10-kW steady-state load. This equates to an average transient load of 2.99 kW for the 10-minute period (Table 5). For the thermal preconditioning case, the steady-state load of 2.1 kW is applied at the start of driving. Additionally, an electric condenser fan is assumed to draw 150 W during the 10-minute transient and 50 W during the steady-state period [7].

2.5.2 Heating

For the electric heating load, it was not possible to define a single load profile for all vehicles because of the different control strategies to use electric power in PHEVs and the availability of waste heat in some vehicles. We reviewed the literature and defined composite electric heating loads for a PHEV15, PHEV40s, and EV. Table 4 shows the vehicle types and environments we considered from a variety of sources.

PHEV15—The electric heaters transition from 4 kW to 0 kW in 10 minutes as waste heat becomes available in the no thermal preconditioning scenario. For the thermal preconditioning scenario, the electric heater is not used. As the vehicle begins to operate in CS mode and the engine operates intermittently, waste heat will be available for cabin heating.

PHEV40s and EV—There is no waste engine heat, and all the heating power is supplied by electric heaters. There is a peak load of 6 kW initially that decreases to 2 kW at 10 minutes (Table 5). For the thermal preconditioning scenario, the 2 kW load is applied at all time points during the simulation.

Table 4: Heating Load Data Sources

Source	Vehicle	Environment
Behr [8]	analysis	cold
ANL [3]	small EV	moderate
GM [9]	conventional	cold
Ford [10]	EV	cold
GM [11]	HEV	cold
Valeo [12, 13, 14]	EV	cold

Table 5: Climate Control Load Profiles

Mode	Vehicle	Peak Load (kW)	Average Transient Load (kW)	Steady-state Load (kW)
A/C	all	3.89	2.99	2.1
heat	PHEV15	4	2	0
heat	PHEV40s and EV	6	4	2

In the development of the SAE mobile A/C life cycle climate performance model, it was assumed that the blower was operated any time the vehicle was operated [15]. Our analysis was consistent with this, and a 150-W blower load was applied during all runs.

2.6 Battery Life

Battery aging is caused by multiple phenomena related to both cycling and calendar age. Battery degradation is accelerated with the depth-of-discharge (DoD) of cycling, elevated temperature, and elevated voltage exposure, among other factors. Worst-case aging conditions drive the need to oversize batteries to meet warranty requirements. Systems and controls, such as thermal preconditioning, may be able to lessen the impact of some of these conditions.

At the battery terminals, the observable effects of degradation are an increase in resistance and a reduction in capacity. These two effects can be correlated with power and energy loss that cause battery end-of-life in an application. Mechanisms for resistance growth include loss of electrical conduction paths in the electrodes, fracture and isolation of electrode sites, growth of film layers at the electrode surface, and degradation of electrolyte. Mechanisms for capacity loss include fracture, isolation, and chemical degradation of electrode material, as well as loss of cyclable lithium (Li) from the system as a byproduct of side reactions.

Under storage or calendar-aging conditions, the dominant fade mechanism is typically growth of a resistive film layer at the electrode surface. As the layer grows, cyclable Li is also consumed from the system, reducing capacity. In the present model, resistance growth and Li-capacity loss are assumed to be proportional to the square-root of time, $t^{1/2}$, typical of diffusion-limited film-growth processes. Under cycling-intense conditions, degradation is mainly caused by structural degradation of the electrode matrix and active sites. Cycling-driven degradation is assumed to be proportional to the number of cycles, N.

Cell resistance growth due to calendar- and cycling-driven mechanisms are assumed to be additive,

$$R = a_0 + a_1 t^{1/2} + a_2 N \quad (3)$$

Cell capacity is assumed to be controlled by either loss of cyclable Li or loss of electrode sites,

$$Q = \min(Q_{Li}, Q_{sites}) \quad (4)$$

where

$$Q_{Li} = b_0 + b_1 t^{1/2}, \text{ and} \quad (5)$$

$$Q_{sites} = c_0 + c_1 N \quad (6)$$

Models (3), (5), and (6) are readily fit to a resistance or capacity trajectory measured over time for one specific storage or cycling condition. Using multiple storage and cycling datasets, functional dependence can be built for rate constants $a_1(T, V, \Delta DoD)$, $a_2(T, V, \Delta DoD)$, $b_1(T, V, \Delta DoD)$, $c_1(T, V, \Delta DoD)$. The present battery life model was fit to laboratory aging datasets [16-19] for the Li-ion graphite/nickel-cobalt-aluminum (NCA) chemistry as described in [19]. The NCA chemistry has generally graceful aging characteristics, and is expected to achieve 8 or more years of life when sized appropriately for a vehicle application.

2.7 Climate Control and Temperature Scenarios

Battery degradation is greatly affected by temperature, both while the vehicle is driving as well as while the vehicle is parked. Battery temperature when parked will be affected by recent driving history, outside ambient conditions, and heat dissipation path to outside ambient conditions where those ambient conditions have strong daily and annual variations. As an initial study, the present work neglects temperature variation due to variable ambient conditions.

Each climate control scenario incorporated an ambient temperature condition. For scenarios that include thermal preconditioning, the battery pack temperature was adjusted from ambient temperature. That is, for thermal preconditioning scenarios, the battery was warmed above a cold ambient temperature or was cooled below a hot ambient temperature over a 20-minute period prior to driving. These climate control, ambient, and battery pack temperature scenarios are presented in Table 6.

Table 6: Climate Control, Temperature Scenarios

Climate Control Scenario	Ambient Temp.	Thermal Preconditioning	Initial Battery Temp.
A/C on (hot)	35°C	yes	26.7°C
		no	35°C
Heat on (cold)	-6.7°C	yes	1.7°C
		no	-6.7°C
Neither A/C nor heat on	20°C	NA	20°C

Twenty-four–hour profiles for battery temperature were created using battery heat generation rates taken from previously described vehicle simulations. As shown in Figure 1, the profiles assume a daily travel distance of 52.8 km/day (33 miles/day), divided into two driving trips, one at 8:00 a.m. and one at 5:00 p.m. Battery charging occurs at 10:00 p.m. at a 6.6-kW rate. For cases with thermal preconditioning, the two daily driving trips are preceded by a 20-minute ramp to the preconditioned temperature.

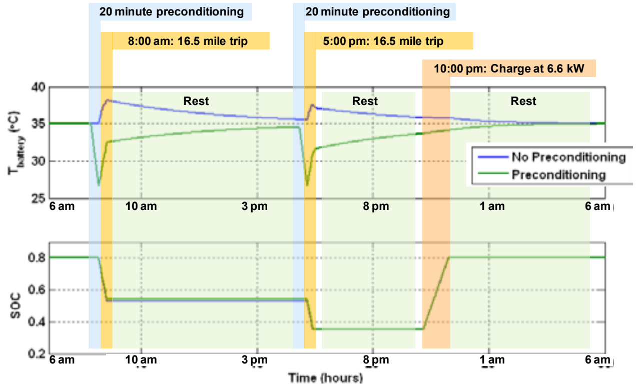

Figure 1: Battery temperature and SOC profiles for PHEV40s, 35°C ambient temperature, with and without thermal preconditioning

3. Results

This section presents the results of vehicle performance and battery life analyses for the range of climate control system usage, ambient and battery temperature, and thermal preconditioning scenarios.

3.1 Vehicle Performance

Fuel consumption and CD range were simulated for each vehicle platform, with and without thermal preconditioning, for each climate control scenario. Results indicate the relatively large impact of climate control on CD range reduction, as well as the benefit of thermal preconditioning in avoiding climate control system-induced battery discharge.

Figure 2 presents results for the PHEV15. This vehicle was modeled to use both engine and battery as needed in a blended fashion. Using heat increases fuel consumption by 3.3% and decreases the CD range by 19.5%. Using A/C increases fuel consumption by 49.3% and decreases the CD range by 32.3%. Thermal preconditioning provides measureable benefits by reducing the initial climate control system load. Compared to no thermal preconditioning, thermal preconditioning with heat decreases fuel consumption by 1.4% and increases CD range by 19.2%. Compared to no thermal preconditioning, thermal preconditioning with A/C decreases fuel consumption by 0.6% and increases the CD range by 5.2%.

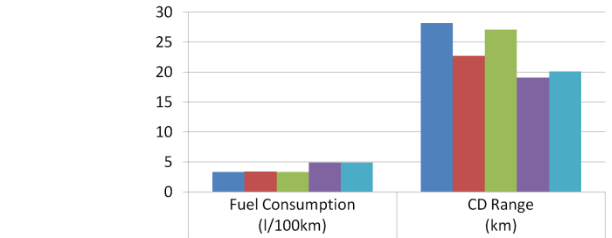

	Fuel Consumption (l/100km)	CD Range (km)
No Climate Control	3.29	28.25
Heat	3.40	22.74
Heat (preconditioned)	3.35	27.11
AC	4.91	19.11
AC (preconditioned)	4.88	20.11

Figure 2: PHEV15 performance

Figure 3 presents results for the PHEV40s. Using heat increases fuel consumption by 60.7% and decreases the CD range by 35.1%. Using A/C increases fuel consumption by 56.8% and decreases the CD range by 34%. Compared to no thermal preconditioning, thermal preconditioning with heat decreases fuel consumption by 2.7% and increases the CD range by 5.7%. Compared to no thermal preconditioning, thermal preconditioning with A/C decreases fuel consumption by 1.5% and increases the CD range by 4.3%.

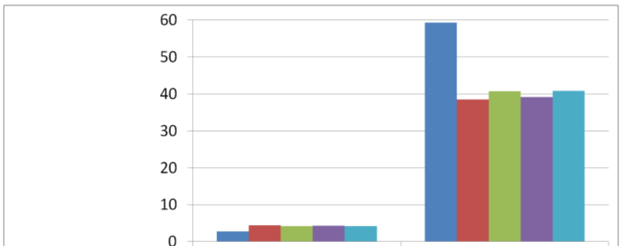

No Climate Control	2.73	59.34
Heat	4.39	38.50
Heat (preconditioned)	4.28	40.69
AC	4.29	39.15
AC (preconditioned)	4.22	40.84

Figure 3: PHEV40s performance

Figure 4 presents results for the EV. Using heat decreases the CD range by 34.7%. Using A/C decreases the CD range by 32.7%. Compared to no thermal preconditioning, thermal preconditioning with heat increases the CD range by 3.9%. Compared to no thermal preconditioning, thermal preconditioning with A/C increases the CD range by 1.7%.

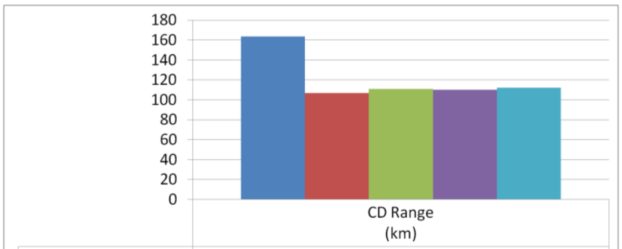

	CD Range (km)
No Climate Control	163.79
Heat	106.98
Heat (preconditioned)	111.14
AC	110.22
AC (preconditioned)	112.06

Figure 4: EV performance

3.2 Battery Life Impacts

Battery 24-hour duty-cycle profiles were input into the life model described in Section 2.5 to simulate battery resistance growth and capacity fade over 10 years. Those results are presented here as a percent-per-year degradation rate. The primary factor causing different battery degradation rates between preconditioned and non-preconditioned cases is the battery temperature exposure. Non-thermally-preconditioned vehicles also experience slightly deeper battery discharges each day, although this is a minor factor in the present battery degradation predictions.

Figure 5 shows percent resistance growth per year (blue bar), percent capacity loss per year (green bar), and battery average temperature (red symbol) for the PHEV15 for the various constant ambient temperatures, with and without preconditioning. For reference, end-of-life is commonly defined when battery remaining capacity has reached 70% to 80% of beginning-of-life capacity. A 2.5% capacity loss per year would result in 80% remaining capacity after 8 years. For example, a 2.0% capacity loss per year in Figure 5 would result in 80% remaining after 10 years. Ambient temperature has the strongest influence on battery degradation rates. Compared to the 20°C baseline case, the 35°C ambient case with no preconditioning increases capacity fade rates by 43%. The −6.7°C ambient case reduces fade by 52% relative to 20°C ambient.

Battery fade rates for actual geographic locations will be a composite of the constant ambient temperatures simulated here. In the United States, Phoenix, Arizona, is a typical worst-case high-temperature location, with annual and daily temperature variation expected to cause battery degradation similar to a 30°C constant temperature aging condition [20].

For the PHEV15 in Figure 5, thermal pre-heating at -6.7°C ambient has a slight negative impact on battery capacity loss, increasing fade rate by 4.5%. At such low temperatures, however, the small fade rates are relatively inconsequential. Hot ambient conditions will derive the most benefit from thermal pre-cooling. At 35°C ambient temperature, pre-cooling decreases the capacity-fade rate by 2.1% for the PHEV15 with air-cooled battery. This reduction in the hot-climate fade rate can be used in either of two ways: (1) if battery size is fixed, a preconditioned battery will last longer than a non-preconditioned battery, or (2) if battery size is not fixed, a preconditioned battery can be sized slightly smaller (with lower cost) and still achieve the same life as a non-preconditioned battery.

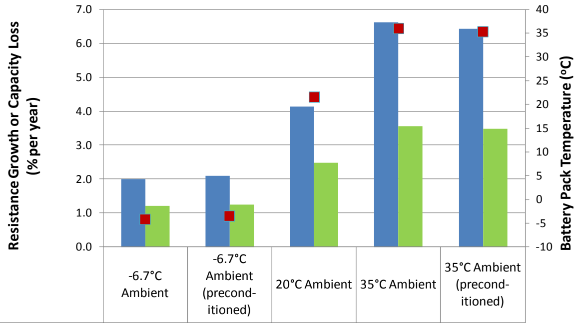

	-6.7°C Ambient	-6.7°C Ambient (precond-itioned)	20°C Ambient	35°C Ambient	35°C Ambient (precond-itioned)
Resistance Growth	2.0	2.1	4.1	6.6	6.4
Capacity Loss	1.2	1.3	2.5	3.6	3.5
Average Temperature	-4.2	-3.4	21.6	35.9	35.2

Figure 5: PHEV15 battery degradation rates (left axis) and average temperature (right axis)

Figure 6 and Figure 7 show battery degradation rates for the PHEV40s and EV platforms, respectively. Trends are similar to the PHEV15. At 35°C ambient, thermal preconditioning reduces capacity-loss rate by 4.1% and 7.1% for the respective PHEV40s and EV platforms. Reductions in resistance-growth rate are 7.0% and 13.8% for the respective platforms.

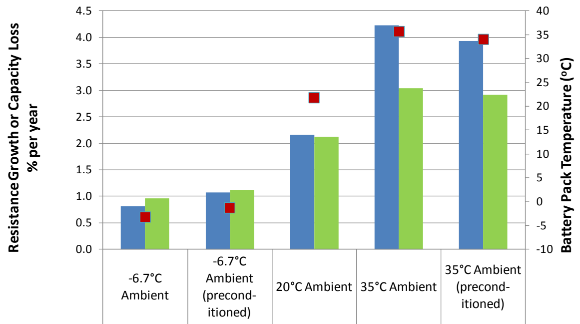

	-6.7°C Ambient	-6.7°C Ambient (precond-itioned)	20°C Ambient	35°C Ambient	35°C Ambient (precond-itioned)
Resistance Growth	0.8	1.1	2.2	4.2	3.9
Capacity Loss	1.0	1.1	2.1	3.0	2.9
Average Temperature	-3.2	-1.3	21.7	35.7	34.0

Figure 6: PHEV40s battery degradation rates (left axis) and average temperature (right axis)

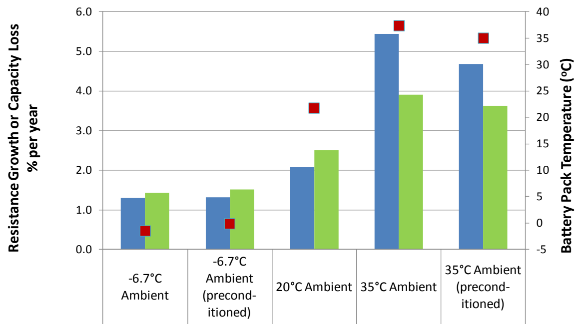

	-6.7°C Ambient	-6.7°C Ambient (precond-itioned)	20°C Ambient	35°C Ambient	35°C Ambient (precond-itioned)
Resistance Growth	1.3	1.3	2.1	5.4	4.7
Capacity Loss	1.4	1.5	2.5	3.9	3.6
Average Temperature	-1.5	-0.2	21.7	37.4	35.0

Figure 7: EV battery degradation rates (left axis) and average temperature (right axis)

In summary, pre-cooling of electric-drive vehicle batteries is predicted to reduce capacity fade by 2.1% to 7.1% and resistance growth by 3.0% to 13.8% in hot (35°C) ambient conditions. In a hot geographic location such as Phoenix, Arizona, (where degradation due to fluctuating ambient temperature is similar to constant 30°C aging), the realized reduction in battery degradation will be slightly less. The three vehicle platforms each derive slightly different benefits from pre-cooling, partly due to the assumed battery thermal management strategies (Table 1) and partly due to the size of each vehicle's battery. Battery temperature rise results from multiple factors, namely battery thermal mass, heat generation rate while driving, and rate of active cooling. Energy storage systems that benefit most from pre-cooling will be those with small battery thermal mass, those with high heat generation rates, and those with limited or no active cooling while driving. Each of these systems is likely to experience a large temperature rise while driving and will benefit from starting a driving trip with a pre-cooled battery.

4. Conclusions

This analysis shows that climate control system loads can significantly increase fuel consumption (up to 60.7%) and decrease CD range (up to 35.1%) in PEVs. Off-board powered thermal preconditioning of a vehicle cabin is one way to reduce the negative impact of climate control system loads. When compared to no thermal preconditioning, thermal preconditioning can provide a moderate reduction in fuel consumption (up to 2.7%). However, thermal preconditioning can partially restore CD range (up to 19.2%). The restoration of several kilometers of CD range may resonate with consumers for whom "range anxiety" is an issue and potential barrier to widespread adoption of PEVs.

Pre-cooling of electric-drive vehicle batteries is predicted to reduce capacity fade by 2% to 7% and resistance growth by 3% to 14% in hot (35°C) ambient conditions. Vehicles that benefit most from battery pre-cooling will be those with small battery thermal mass or high heat generation rates (i.e., PHEVs with a short electric range) and those with limited battery active cooling systems.

Off-board powered thermal preconditioning has benefits to the consumer via CD range extension and less expensive energy costs (electricity versus liquid fuel and/or battery capacity), as well as vehicle manufacturers via extended battery life and avoided warranty claims.

5. References

[1] Gonder, J., Brooker, A., Carlson, R., and Smart, J. *Deriving In-Use PHEV Fuel Economy Predictions from Standardized Test Cycle Results,* presented at the 5th IEEE Vehicle Power and Propulsion Conference, Dearborn, Michigan, 2009 (NREL/CP-540-46251).

[2] *Society of Automotive Engineers, Cooperative Research Program: Alternative Refrigerant Project Phase I, Draft Final Report,* July 14, 2003.

[3] Lohse-Busch, H., *Small EV Testing and Analysis*, Presentation to DOE. Argonne National Laboratory November 17, 2009. email re: Test data, APRF.

[4] Rugh, J. (2009). *Impact of Sungate EP on PHEV Performance: Results of a Simulated Solar Reflective Glass PHEV Dynamometer Test.* 32 pp.; NREL Report No. TP-540-45908. Golden, CO: National Renewable Energy Laboratory.

[5] Maranville, C., Ford Motor Company, personal email. Ford Fusion cooling load. June 4, 2010.

[6] Meyer, J., Visteon Corporation, A/C Cooling Load data, March 1, 2007.

[7] Papasavva, S., Hill, W.R., and Brown, R.O., "GREEN-MAC-LCCP®: A Tool for Assessing Life Cycle Greenhouse Emissions of Alternative Refrigerants," Proceedings of the 2008 SAE Congress, Detroit, MI. Paper # 2008-01-0829. Society of Automotive Engineers.

[8] Feuerecker, G., Schafer, B, Strauss, and T. Behr., "Auxiliary Heating Systems of Conventional and Heat Pump Type: Technology, Performance, and Efficiency," Proceedings of the 7th Vehicle Thermal Management Systems Conference, May 10-12, 2005, Toronto, Canada, Paper # 2005-01-2055, Society of Automotive Engineers. 2005-01-2055 SAE.

[9] Hill, W. Retired from GM, personal communication, June 15, 2010.

[10] Maranville, C. Ford Motor Company, personal communication, June 4, 2010.

[11] Zeng, X., Major, G., Hirao, T., and Imaiida, T., "An Automotive Hybrid Heating System for Parallel Hybrid Passenger Cars," Proceedings of the 2000 SAE Congress, Detroit, MI., March, 2000, Paper # 2000-01-1276.

[12] Roy, D., Petitjean, P., Clodic, D., and El Khoudy, K., "Influence of Thermal Preconditioning technologies on A/C System Power and Passenger Thermal Comfort," , Proceedings of the 6th Vehicle Thermal Management Systems Conference, May 18-21, 2001, Brighton, UK, Paper # C599/004/2003.

[13] Dauvergne, J., "Thermal Comfort of Electric Vehicles," Proceedings of the 1994 SAE Congress, Detroit, MI. March 1994, Paper #. 940295. Society of Automotive Engineers. Society of Automotive Engineers.

[14] Pomme, V., "Reversible Heat Pump System for an Electrical Vehicle," Proceedings of the 1997 SAE Congress, Detroit, MI. May 1997, Paper #..971772, Society of Automotive Engineers.

[15] SAE J 2766 SURFACE VEHICLE STANDARD "Life Cycle Analysis to Estimate the CO2-Equivalent Emissions from MAC Operation," issued February 16, 2009.

[16] Broussely, M., "Aging of Li-ion batteries and life prediction, an update," 3rd Int. Symposium on Large Lithium-Ion Battery Technology and Application, Long Beach, California, May 2007.

[17] Hall, J., Lin, T., Brown, G., Biensan, P., and Bonhomme, F., "Decay processes and life predictions for lithium ion satellite cells," 4th Int. Energy Conversion Engineering Conf., San Diego, California, June 2006.

[18] Smart, M., Chin, K., Whitcanack, L., and Ratnakumar, B., "Storage characteristics of Li-ion batteries," NASA Battery Workshop, Huntsville, Alabama, Nov. 2006.

[19] Broussely, M., Chap. 13 in: *Advances in Lithium-Ion Batteries,* van Schalkwijk, W., and Scrosati, B., editors. New York: Kluwer Academic / Plenum Publishers, 2002.

[20] Smith, K., Markel, T., and Pesaran, A., "PHEV Battery Trade-off Study and Standby Thermal Control," 26th International Battery Seminar & Exhibit, Fort Lauderdale, FL, March, 2009.

6. Acknowledgments

The authors wish to thank Lee Slezak and David Anderson, U.S. Department of Energy Vehicle Technologies Program, for their financial support in conducting this project.

7. Authors

Robb A. Barnitt
National Renewable Energy Laboratory
Golden, Colorado USA
Email: robb.barnitt@nrel.gov
Mr. Barnitt leads Vehicle Systems Analysis staff and research within the Center for Transportation Technologies and Systems at NREL. He holds a B.S. from the University of Massachusetts at Amherst and a M.S. in engineering from Stanford University.

Aaron Brooker
National Renewable Energy Laboratory
Golden, Colorado USA
Email: aaron.brooker@nrel.gov
Mr. Brooker is a Senior Engineer at the National Renewable Energy Laboratory. He holds a B.S. in mechanical engineering from Michigan Technological University (1998) and a M.S. in mechanical engineering from the University of Colorado (2000).

Laurie Ramroth
National Renewable Energy Laboratory
Golden, Colorado USA
Email: laurie.ramroth@nrel.gov
Ms. Ramroth is an Engineer at the National Renewable Energy Laboratory. She holds a B.S. in mechanical engineering from Wayne State University in Detroit, Michigan, where she focused on alternative energy technologies.

John Rugh
National Renewable Energy Laboratory
Golden, Colorado USA
Email: john.rugh@nrel.gov
Mr. Rugh is a Senior Engineer at NREL, where he leads CoolCab and Vehicle Integrated Thermal Management tasks. He holds a B.S. in mechanical engineering from Colorado State University and an M.S. in mechanical engineering from Purdue University.

Kandler A. Smith
National Renewable Energy Laboratory
Golden, Colorado USA
Email: kandler.smith@nrel.gov
Dr. Smith is a senior engineer researching energy storage systems for NREL's Center for Transportation Technologies. He holds a Ph.D. degree in mechanical engineering from Pennsylvania State University. He is an active member of the IEEE, the Electrochemical Society, and the Society for Automotive Engineers. His research includes electric-drive vehicles, battery electrochemical/thermal characterization and modeling, and battery-life predictive modeling.

REPORT DOCUMENTATION PAGE	*Form Approved* *OMB No. 0704-0188*

1. **REPORT DATE** *(DD-MM-YYYY)*	2. **REPORT TYPE**	3. **DATES COVERED** *(From - To)*
December 2010	Conference Paper	

4. **TITLE AND SUBTITLE** Analysis of Off-Board Powered Thermal Preconditioning in Electric Drive Vehicles: Preprint	5a. **CONTRACT NUMBER** DE-AC36-08GO28308
	5b. **GRANT NUMBER**
	5c. **PROGRAM ELEMENT NUMBER**
6. **AUTHOR(S)** R.A. Barnitt, A.D. Brooker, L. Ramroth, J. Rugh, and K.A. Smith	5d. **PROJECT NUMBER** NREL/CP-5400-49252
	5e. **TASK NUMBER** FC10.2400
	5f. **WORK UNIT NUMBER**
7. **PERFORMING ORGANIZATION NAME(S) AND ADDRESS(ES)** National Renewable Energy Laboratory 1617 Cole Blvd. Golden, CO 80401-3393	8. **PERFORMING ORGANIZATION REPORT NUMBER** NREL/CP-5400-49252
9. **SPONSORING/MONITORING AGENCY NAME(S) AND ADDRESS(ES)**	10. **SPONSOR/MONITOR'S ACRONYM(S)** NREL
	11. **SPONSORING/MONITORING AGENCY REPORT NUMBER**

12. **DISTRIBUTION AVAILABILITY STATEMENT**
National Technical Information Service
U.S. Department of Commerce
5285 Port Royal Road
Springfield, VA 22161

13. **SUPPLEMENTARY NOTES**

14. **ABSTRACT** *(Maximum 200 Words)*
Following a hot or cold thermal soak, vehicle climate control systems (air conditioning or heat) are required to quickly attain a cabin temperature comfortable to the vehicle occupants. In a plug-in hybrid electric or electric vehicle (PEV) equipped with electric climate control systems, the traction battery is the sole on-board power source. Depleting the battery for immediate climate control results in reduced charge-depleting (CD) range and additional battery wear. PEV cabin and battery thermal preconditioning using off-board power supplied by the grid or a building can mitigate the impacts of climate control. This analysis shows that climate control loads can reduce CD range up to 35%. However, cabin thermal preconditioning can increase CD range up to 19% when compared to no thermal preconditioning. In addition, this analysis shows that while battery capacity loss over time is driven by ambient temperature rather than climate control loads, concurrent battery thermal preconditioning can reduce capacity loss up to 7% by reducing pack temperature in a high ambient temperature scenario.

15. **SUBJECT TERMS**
EV; PEV; PHEV; thermal; climate control

16. **SECURITY CLASSIFICATION OF:**			17. **LIMITATION OF ABSTRACT**	18. **NUMBER OF PAGES**	19a. **NAME OF RESPONSIBLE PERSON**
a. **REPORT**	b. **ABSTRACT**	c. **THIS PAGE**			
Unclassified	Unclassified	Unclassified	UL		19b. **TELEPHONE NUMBER** (*Include area code*)